

THE p–C ANALYZING POWER BETWEEN 100 AND 750 MeV *

M.W. McNAUGHTON, B.E. BONNER, H. OHNUMA **, O.B. VAN DIJK and SUN TSU-HSUN +
Los Alamos National Laboratory, Los Alamos, NM 87545, USA

C.L. HOLLAS, D.J. CREMANS, K.H. MCNAUGHTON, P.J. RILEY, R.F. RODEBAUGH and
SHEN-WU XU

University of Texas at Austin, Austin, TX 78712, USA

S.E. TURPIN

Rice University, Houston, TX 77251, USA

B. AAS and G.S. WESTON

University of California at Los Angeles, Los Angeles, CA 90024, USA

Received 11 February 1985

The inclusive p–C analyzing power has been measured for laboratory scattering angles between 3° and 19° for energies between 80 and 584 MeV. The experiment was performed at LAMPF using a large solid angle polarimeter. These data have been incorporated into the existing data base to obtain a new energy dependent p–C analyzing power fit for the energy range 100–750 MeV.

1. Introduction

Accurate values of the analyzing power A_c in inclusive proton–carbon scattering are essential in determining the scattered proton polarization, and hence, in extracting pp elastic and inelastic spin depolarization parameters. Ransome et al. [1,2] parameterized A_c as a function of θ_{lab} , the laboratory scattering angle in carbon, and E_{carb} , the mean energy at the carbon center. Since then, more inclusive proton–carbon analyzing power measurements have been carried out. We have incorporated these recent measurements into the data base used by Ransome et al. [1], and have obtained a new energy-dependent p–C analyzing power fit for the energy range 100–750 MeV. The new fit reduces the overall error to $\approx 2\%$, and significantly improves the parameterization for E_{carb} values between 100 and 140 MeV.

* This work was supported in part by the US Department of Energy.

** Present address: Tokyo Institute of Technology, Oh-okayama, Tokyo 152, Japan.

+ On leave from Institute of Atomic Energy, Academia Sinica, Peking, People's Republic of China.

2. Experimental method

The experimental method is as described by Ransome et al. [1]. As in their measurements, the polarimeter Janus, consisting of a scintillator, three drift chambers, an analyzer, three more drift chambers, and a final scintillator, was used. The carbon analyzer was 60 cm square and varied in thickness between 3.17 and 25.4 cm. The measurements were performed either in the polarized beam directly from the LAMPF accelerator (LZ type data), or with protons polarized by elastic scattering from a liquid hydrogen target and relying on the knowledge of the elastic pp polarizing power to determine the scattered beam polarization (LE type data). The data are tabulated in table 1.

3. Results and energy dependent fit

We use the same parameterization of the analyzing power that was used by Ransome et al. The energy range is divided at 450 MeV into a “low energy region” and a “high energy region”. For the low energy fit, the fitting function used is

$$A_c(\theta_{lab}, E_{carb}) = \frac{ar}{1 + br^2 + cr^4}. \quad (1)$$

For energies greater than about 450 MeV, an additional term is included, so that the functional form of the “high energy fit” is

$$A_c(\theta_{\text{lab}}, E_{\text{carb}}) = \frac{ar}{1 + br^2 + cr^4} + dp \sin(5\theta_{\text{lab}}). \quad (2)$$

In both cases $r = p \sin(\theta_{\text{lab}})$, where p is the momentum at the carbon center in GeV/ c . Furthermore, an energy-dependent polynomial fit is used for the param-

eters a , b , c , and d . For the low energy fit,

$$a = a_0 + a_1 p' + a_2 p'^2 + a_3 p'^3 + a_4 p'^4,$$

$$b = b_0 + b_1 p' + b_2 p'^2 + b_3 p'^3 + b_4 p'^4,$$

and

$$c = c_0 + c_1 p' + c_2 p'^2 + c_3 p'^3 + c_4 p'^4,$$

where $p' = p - 0.7$ GeV/ c . For the high energy fit, a

Table 1
Recent LAMPF inclusive *p*-C analyzing power measurements

θ_{lab}	584 MeV ^{a)}		562 MeV ^{a)}		518 MeV ^{a)}	
	A_c	ΔA_c	A_c	ΔA_c	A_c	ΔA_c
3.15	0.177	0.026	0.156	0.028	0.170	0.024
3.72	0.201	0.027	0.191	0.029	0.214	0.025
4.32	0.242	0.027	0.260	0.029	0.257	0.026
5.18	0.254	0.021	0.287	0.022	0.270	0.019
6.30	0.342	0.025	0.297	0.024	0.297	0.020
7.45	0.304	0.025	0.339	0.026	0.344	0.022
8.60	0.312	0.028	0.334	0.030	0.368	0.025
9.78	0.294	0.031	0.345	0.034	0.314	0.029
11.24	0.275	0.030	0.254	0.033	0.302	0.028
13.27	0.227	0.030	0.198	0.035	0.231	0.030
15.88	0.245	0.034	0.209	0.039	0.226	0.034
18.61	0.211	0.042	0.219	0.050	0.252	0.043
θ_{lab}	470 MeV ^{a)}		415 MeV ^{a)}		171 MeV ^{a)}	
	A_c	ΔA_c	A_c	ΔA_c	A_c	ΔA_c
3.15	0.172	0.028	0.204	0.035		
3.72	0.208	0.030	0.194	0.041		
4.32	0.190	0.030	0.282	0.043		
5.18	0.281	0.022	0.341	0.031		
6.27					0.364	0.057
6.30	0.336	0.024	0.403	0.033		
7.45	0.325	0.026	0.469	0.036	0.427	0.059
8.60	0.422	0.028	0.522	0.039		
8.63					0.487	0.060
9.78	0.368	0.033	0.412	0.044		
9.80					0.498	0.062
11.24	0.374	0.032	0.426	0.042	0.537	0.057
13.27	0.279	0.034	0.297	0.046	0.651	0.057
15.84					0.527	0.070
15.88	0.230	0.039	0.300	0.053		
18.51					0.485	0.103
18.61	0.139	0.050	0.228	0.069		
θ_{lab}	128 MeV ^{a)}					
	A_c	ΔA_c				
6.28	0.335	0.058				
7.47	0.425	0.058				
8.62	0.258	0.059				
9.80	0.347	0.061				
11.26	0.388	0.052				
13.27	0.282	0.052				
15.83	0.476	0.061				
18.46	0.290	0.096				

Table 1 (continued)

θ_{lab}	286 MeV ^{c)}		79 MeV ^{b)}	
	A_c	ΔA_c	A_c	ΔA_c
5.2	0.349	0.017		
6.3	0.462	0.016		
7.4			0.057	0.025
7.5	0.493	0.016		
8.6	0.565	0.016	0.085	0.029
9.8	0.579	0.016	0.207	0.029
11.3	0.567	0.014	0.185	0.024
13.3	0.500	0.013	0.174	0.022
15.9			0.187	0.024
16.1	0.420	0.013		
18.6			0.174	0.030

a) LE [3] data taken March 1981. Incident beam energy 647 MeV.

b) LE [3] data taken September 1982. Incident beam energy 750 MeV.

c) LZ [3] data taken January 1983. Incident beam energy 318 MeV. All LE data has been renormalized, as described in the text, in order to correct for instrumental asymmetries.

Table 2
Data base for high energy fit ^{a)}

E_{carb} (MeV)	Source	Carbon thickness (cm)	Range of θ_{lab} (degrees)	Number of points
754.0	LZ[1]	25.4	2.9–33.5	12
747.0	LH[5]	27.0	5.0–18.5	11
707.0	LE[1]	25.4	3.15–18.75	12
693.0	LH[5]		4.0–18.5	12
691.0	LZ[1]	25.4	2.9–29.7	11
676.0	LE[1]	25.4	3.15–18.75	12
620.0	LE[1]	25.4	3.15–18.75	12
587.0	LZ[1]	25.4	2.9–29.7	11
584.0	LE[3]		3.15–18.61	12
582.0	LE[1]	12.7	3.15–18.75	12
571.0	S[6]	5.0	5.5–19.5	15
568.0	S[6]	7.0	5.5–19.5	15
562.0	LE[3]	12.7	3.15–18.61	12
561.0	S[7]	5.0	5.25–19.75	30
541.0	LZ[1]	12.7	2.9–29.7	11
520.0	S[6]	7.0	5.5–19.5	15
518.0	LE[3]	12.7	13.5–18.62	12
512.0	LZ[1]	12.7	5.0–29.7	10
511.0	LE[1]	12.7	3.15–18.75	12
483.0	S[7]	5.0	5.25–19.75	30
475.0	S[6]	7.0	5.5–19.5	15
473.0	LH[4]	12.0	4.0–18.5	12
470.0	LE[3]	12.7	3.15–18.61	12
450.0	T[8]	6.0	4.0–28.0	13
434.0	S[6]	7.0	7.5–19.5	13
427.0	S[6]	7.0	5.5–19.5	15
415.0	LE[3]	12.7	3.14–18.6	12
387.2	T[8]	6.0	4.0–28.0	13
386.0	S[6]	3.0	5.5–19.5	15

a) E_{carb} is the mean energy at the carbon center. See text for explanation of source codes. θ_{lab} is the laboratory scattering angle in the carbon analyzer.

third order polynomial is used, so that

$$a = a_0 + a_1 p' + a_2 p'^2 + a_3 p'^3,$$

$$b = b_0 + b_1 p' + b_2 p'^2 + b_3 p'^3,$$

$$c = c_0 + c_1 p' + c_2 p'^2 + c_3 p'^3,$$

$$d = d_0 + c_1 p' + c_2 p'^2 + c_3 p'^3,$$

where $p' = p - 1.2 \text{ GeV}/c$.

Tables 2 and 3 show the respective data bases used

for the high and low energy fits. The data sets are coded in the same manner as in ref. [1], but with specific references for sources given in the parentheses. LZ and LE indicate LAMPF data obtained from the direct (zero degree) and scattered beam methods, respectively, described by Ransome et al. [1]. Recent LAMPF data from scattered beam measurements are coded LE [3]. Other sources are LH for LAMPF data [4,5] S for SIN data [6,7], and T for TRIUMF data [8].

The data base included all the data tabulated in ref.

Table 3
Data base for low energy fit ^{a)}

E_{carb} (MeV)	Source	Carbon thickness (cm)	Range of θ_{lab} (degrees)	Number of points
483.0	S[7]	5.0	5.25–19.75	30
475.0	S[6]	7.0	5.5–19.5	15
470.0	LE[3]	12.7	3.15–18.61	12
450.0	T[8]	6.0	4.0–28.0	13
434.0	S[6]	7.0	7.5–19.5	13
427.0	S[6]	7.0	5.5–19.5	15
415.0	LE[3]	12.7	3.14–8.6	12
387.2	T[8]	6.0	4.0–28.0	13
386.0	S[6]	3.0	5.5–19.5	15
384.0	S[6]	7.0	5.5–19.5	15
380.0	S[7]	5.0	5.25–19.75	30
357.0	T[8]	6.0	4.0–28.0	13
350.0	S[6]	5.0	5.5–19.5	15
347.0	S[6]	3.0	5.5–19.5	15
345.0	S[6]	7.0	5.5–19.5	15
319.0	T[8]	6.0	4.0–28.0	13
311.0	S[6]	3.0	5.5–19.5	15
300.0	S[6]	7.0	5.5–19.5	15
299.0	S[7]	4.0	5.25–19.75	30
286.0	LZ[3]	9.5	5.2–16.1	8
281.0	S[6]	3.0	5.5–19.5	15
279.0	T[8]	6.0	4.0–28.0	13
275.0	S[6]	5.0	5.5–19.5	15
269.0	S[6]	7.0	5.5–19.5	15
242.0	T[8]	6.0	4.0–28.0	13
234.0	LE[1]	6.4	5.18–18.75	9
225.0	S[6]	7.0	5.5–19.5	15
215.0	S[6]	7.0	5.5–19.5	15
210.0	T[8]	6.0	4.0–28.0	13
179.0	T[8]	6.0	6.0–26.0	11
179.0	S[6]	7.0	6.5–19.5	14
171.0	LE[3]	6.35	6.25–18.51	8
161.0	LE[1]	6.4	6.4–18.76	8
157.0	T[8]	3.0	6.0–26.0	11
145.0	T[8]	6.0	8.0–26.0	10
144.0	S[6]	3.0	6.5–19.5	14
133.0	T[8]	3.0	6.0–26.0	11
128.0	LE[3]	2.9	6.28–18.44	8
119.0	T[8]	6.0	8.0–26.0	10
113.0	T[8]	3.0	6.0–22.0	9
107.0	LE[1]	3.2	8.63–18.76	6
95.0	S[6]	3.0	6.5–19.5	14

^{a)} See text and table 1 for explanation.

[1] with the exception of those data sets coded in that paper as 440 LE, 310 LE, 374 LH, and 304 LH. The first two of those sets were obtained using protons elastically scattered from a liquid-hydrogen target near 90° center of mass, where the elastic proton-proton polarizing power P is close to zero and changes rapidly with angle. The 374 LH and 304 LH sets are early, preliminary LAMPF HRS data [4] and with the availability of more precise data, have been deleted. Recent LAMPF HRS data, however, at 747 and 693 MeV have been included in the present fit [5]. The 747 LH [5] data replace the preliminary 747 LH data listed in ref. [1].

New LE type data and one set of LZ type data [3] have been included in the data base for the high and low energy fits. In addition, all LE type data have been renormalized in order to take instrumental asymmetries into account [3]. Aprile-Giboni et al. [6] reported recent *p*-C analyzing power measurements made at SIN at 25 energies ranging from 95 to 570 MeV. Data at 21 of these energies have now been incorporated into the fit. Four data sets, at energies of 151, 187, 194, and 238 MeV, were not added to the low energy data base because the thickness of the carbon analyzers for these measurements, as a function of the energy in the carbon, did not conform to the standard choices of carbon thickness used for the LAMPF data [9].

Aprile-Giboni et al. [6] also parameterize their *p*-C analyzing power data using an empirical formula similar to eq. (2). However, the SIN group includes an empirical damping factor in order to reproduce the sharp drop of A_c at small values of θ_{lab} induced by multiple Coulomb scattering at low energies. For data taken at LAMPF, the practice is to exclude small angle scatters in the carbon through software cuts. Consequently, the SIN data points at $\theta_{lab} = 5.5^\circ$ have been deleted from the 179, 144, and 95 MeV data sets.

Fig. 1 shows the results of the new *p*-C analyzing power fits in terms of “an average analyzing power”,

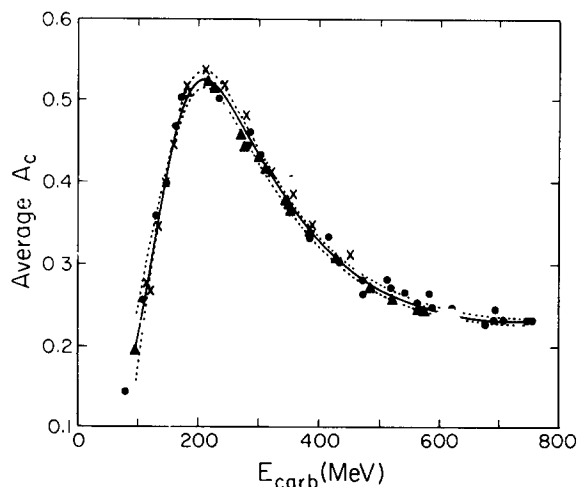


Fig. 1. Single energy (points) and energy dependent (solid line) \bar{A}_c from $\theta_{lab} = 5^\circ$ – 20° are plotted. Data points are from SIN (Δ), TRIUMF (\times), and LAMPF (\bullet). Dotted lines show estimated error corridor.

A_c . A_c is calculated by numerically integrating the appropriate fit for values of θ_{lab} between 5° and 20° , giving equal weight to each angle. The solid line is a graph of A_c versus the mean energy at the carbon center as determined from the polynomial fits with the coefficients found from the updated data base; these coefficients are listed in table 4. The dotted curves demarcate the estimated error corridor of the fit. Data points plotted are the single energy averages.

Analyzing power data at energies from approximately 480 to 385 MeV were included in both the high and low energy data bases in order to facilitate a smooth transition between the two fitting functions. Values of A_c calculated from both the high and low energy dependent fits agree to within a few tenths of a percent between 400 and 500 MeV. In fig. 1, values of

Table 4
Coefficients for low energy (eq. (1)) and high energy (eq. (2)) function

Low energy: number of points = 579, total $\chi^2 = 889.5$					
	0	1	2	3	4
<i>a</i>	5.3346	-5.5361	2.8353	61.915	-145.54
<i>b</i>	-12.774	-68.339	1333.5	-3713.5	3738.3
<i>c</i>	1095.3	949.50	-28012.0	96833.0	-118830.0
High energy: number of points = 399, total $\chi^2 = 514.7$					
	0	1	2	3	
<i>a</i>	1.6575	1.3855	9.7700	-149.27	
<i>b</i>	-16.346	152.53	139.16	-3231.1	
<i>c</i>	1052.2	-3210.8	-2293.3	60327.0	
<i>d</i>	0.13887	-0.19266	-0.45643	8.1528	

A_c from the “low energy fit” are used up to 450 MeV, and from the “high energy fit” for energies in the carbon of 450 MeV and above. No discontinuity is evident at the dividing energy.

4. Conclusions

The mean and standard deviation of the χ^2 per point are plotted in energy bins of 200 MeV in fig. 2 for the LAMPF, SIN, and TRIUMF data sets. In the 400 MeV $< E_{\text{carb}} < 600$ MeV bin, the only TRIUMF data set is T 450 [8] with a χ^2 per point of 1.61. This point is plotted in fig. 2 for comparison. Also, only two LAMPF data sets, 286 LZ [3] (χ^2 per point = 1.72) and 234 LE [1] (χ^2 per point = 1.67), fell in the 200–400 MeV bin.

The current fit has a somewhat smaller overall χ^2 for the higher, as compared with the lower, E_{carb} data. Although the relatively large standard deviations show a wide variation of χ^2 per point among data sets, it does not appear that data from any one of the three laboratories fit significantly worse than the other data.

Fig. 3 shows a comparison between the present updated fit and the earlier fit of Ransome et al. The two curves agree within 1.2% or better down to $E_{\text{carb}} = 140$ MeV, although the new fit is systematically lower than

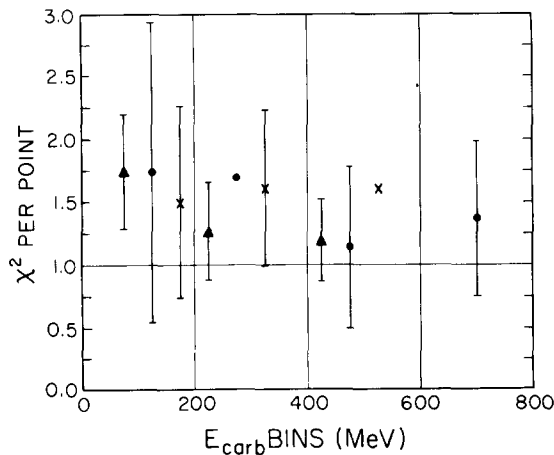


Fig. 2. Mean and standard deviation of χ^2 per point for energy dependent fit of SIN (Δ), TRIUMF (\times), and LAMPF (\bullet) data averaged in E_{carb} bins of 200 MeV.

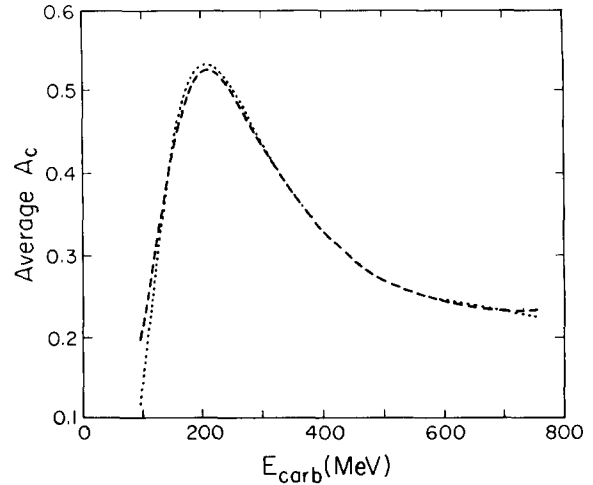


Fig. 3. Energy dependent \bar{A}_c are calculated using current coefficients (dashed curve) and coefficients of ref. [1] (dotted curve).

the previous one in this range. This shift, however, is comfortably within the error corridor of $\pm 2.5\%$ estimated for the fit of Ransome et al. above 200 MeV. With the expanded data bases, the estimated error corridor of the present energy dependent fit is $\pm 2\%$ for $E_{\text{carb}} \geq 140$ MeV. Less than one-eighth of the single energy fits above 140 MeV fail to overlap this corridor.

The most significant difference between the two fits occurs for E_{carb} below about 140 MeV. The old fit drops too sharply in this region, and in fact, gives an energy dependent A_c for the 95 S [6] data that is about 40% too low.

References

- [1] R.D. Ransome et al., Nucl. Instr. and Meth. 201 (1982) 315.
- [2] R.D. Ransome, Los Alamos National Laboratory Report LA-8919-T.
- [3] M.W. McNaughton, private communication.
- [4] J.B. McClelland, private communication.
- [5] M. Barlett, private communication.
- [6] E. Aprile-Giboni et al., Nucl. Instr. and Meth. 215 (1983) 147.
- [7] D. Besset et al., Nucl. Instr. and Meth. 166 (1979) 379.
- [8] G. Waters et al., Nucl. Instr. and Meth. 153 (1978) 401.
- [9] R.D. Ransome et al., Nucl. Instr. and Meth. 201 (1982) 309.